Journal of Sound and Vibration (2002) **251**(1), 1–12
doi:10.1006/jsvi.2001.3806, available online at http://www.idealibrary.com on IDEAL®

A MATHEMATICAL MODEL FOR WIND TURBINE BLADES

A. Baumgart

Forskningscenter Risø, Prøvestationen for Vindmøller, Postboks 49, *DK*-4000 *Roskilde, Denmark.*
E-mail: abau@germanlloyd.org

(*Received* 14 *February* 2000, *and in final form* 21 *March* 2001)

A mathematical model for an elastic wind turbine blade mounted on a rigid test stand is derived and compared with experimental results. The linear equations of motion describe small rotations of the test stand, blade lateral deflections and rotation of the chord. Warping, extension and tilt of the cross-sections are slaved to the dependent minimal co-ordinates in order to reduce the number of state variables. Using the principle of virtual work, a procedure is employed which combines the volume discretization of general "solid", or shell-type finite elements (FE), with the approach of global form functions (stretching over the whole blade length). The equations of motion are solved as an eigenvalue problem and the results are compared with an experimental modal analysis of a 19 m long blade. The computed eigenfrequencies fit well, but the mathematical model underestimates the pitch motion of the blade chord. Parameter studies show the effect of warping. Despite the few degrees of freedom and uncertainties in the model parameters, the mathematical model approximates the measured blade dynamics well.

1. INTRODUCTION

Rod models, such as beams and strings, have essentials advantages compared with general solid or shell-type finite-element (FE) models when describing slender solid bodies. The co-ordinates are intuitively related to the motion of the physical system, significantly fewer degrees of freedom can be chosen and the range of eigenvalues is restricted to the relevant low frequencies.

However, all well-known rod models are limited to symmetric cross-sections. They can be extended to account, e.g., for elastic or inertia coupling of bending and torsion, but supplementary information like the location of shear centre, mass centre or the principal bending axes need then to be given. The equations of motion for the rod are derived from equilibrium considerations.

In wind turbine simulation programs these rod models are widely used. In reference [1], the differential equations for a rotating blade from reference [2] are employed, describing elastic and inertia coupling of bending and torsion. However, potential transverse shear effects, due to a high ratio of in-plane modulus to transverse shear in turbine blades made from composites, are not accounted for. Another drawback of these models is the need to compute cross-sectional properties like shear centre, tension centre, etc. from more refined models which take warping into account. In reference [3], a procedure is proposed that computes this supplementary information for cylindrical segments of cross-sections of wind turbine blades with the warping function as the primary unknown.

A different approach employs variational principles to derive the equations of motion under appropriate assumptions for the relevant deformation mechanisms of the rod. For

0022-460X/02/110001 + 12 $35.00/0

Euler–Bernoulli or Timoshenko beams this assumption would be that an initially plain cross-section remains plain under deformation (an assumption which does not hold for a blade, because warping *is* relevant). These dedicated assumptions lead to a reduction in the number of independent spatial variables in the equations of motion from three to one. By computing the stresses from the assumed displacements, the strains and thus the virtual work of the rod can be computed.

In reference [4] an example is given for a cylindrical beam with open cross-section where warping is chosen according to the Vlasov thin-walled beam theory. The equations of motion are derived using the principle of virtual work.

Hamilton's principle is employed in reference [5] when deriving the rod equations of motion using a higher-order theory. To approximate the axial and transverse displacements of the cross-section, a Taylor series expansion is chosen. The model accounts for orthotropic material characteristics. A thorough introduction into the related literature is given.

In this article, a blade model based on similar assumptions as in reference [5] is presented. The axial and transverse displacements of points on a cross-section result from a series of cross-sectional displacements, rotations and deformations which are associated with respective dependent co-ordinates. The principle of virtual work is employed. The model combines the flexibility of shell- or solid-type FE discretization of the structure with the simplicity of rod models: the form functions are global polynomials over the whole blade length, whereas the blade structure is subdivided into finite hexahedra. The virtual work of the system is computed numerically by summation over the virtual work of all hexahedra. The self-contained method can be applied to general slender rods with closed cross-sections.

Vector calculus is employed for a straightforward description of the blade motion. Since the blade is not rotating as in operation on a wind turbine, no gyroscopic terms were accounted for. Nevertheless, the method can be, and has been, extended to derive the kinetic energy for a rotating blade (see, e.g., [reference 6, Section 6.4.5]).

The intention of this article is to justify the development of a rod model for wind turbine blades for applications where a significant reduction in the number of co-ordinates with respect to general FE models is needed, e.g., when used in simulations in the time domain and/or systematic stability investigations of wind turbines.

2. EQUATIONS OF MOTION

A mathematical model for a flexible wind turbine blade is derived. The blade is mounted on a rigid test stand S. At O, the test stand is elastically supported allowing for rotation only (see Figure 1). The strainless reference configuration is defined so that the blade reference axis R is horizontal and the blade chord is vertical near the tip. The blade is 19 m long, its maximum chord length is 1·7 m and the trailing edge points upwards. O and B are points on R, where B is a point on the blade root cross-section and where $\overline{OB} = b$.

The expression "cross-section z" identifies all material points which hold a position in plane z perpendicular to R, when the blade is in its undeformed reference configuration. "Profile" refers to the outer circumference of a cross-section. A motion is called "flapwise" when it is predominantly horizontal, "edgewise" refers to vertical motion and "pitchwise" to chord rotation.

Throughout the text an underlined symbol, e.g., $\underline{r}$, represents a column matrix and a bold-faced symbol, e.g., $\mathbf{r}$, a vector. A column matrix is a triple of elements, a vector is an element of the three-dimensional space. Thus, in $\mathbf{r} = \underline{r}\ \underline{\mathbf{e}}_I\ \mathbf{r}$ is the line element spanned between the origin and a point in space and $\underline{r}$ gives the point's co-ordinates in the

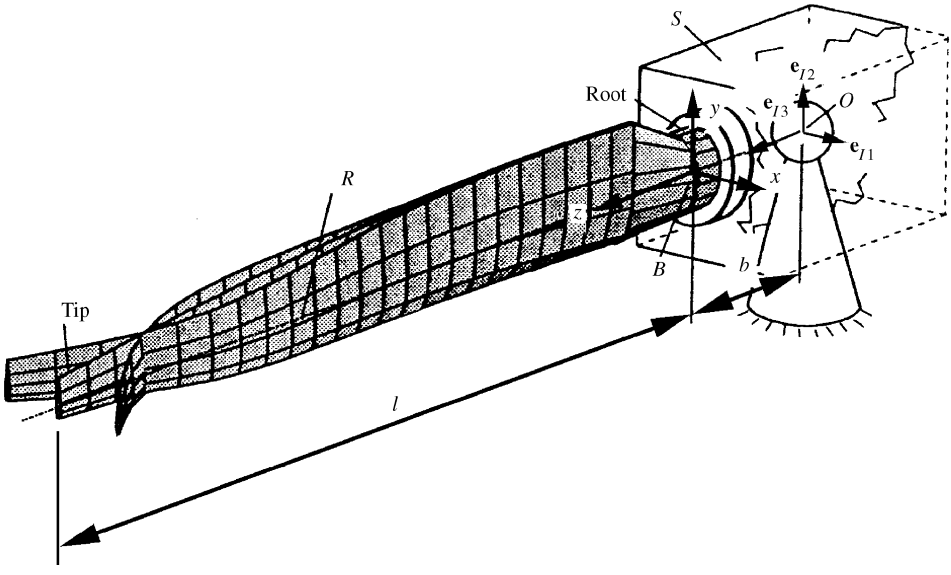

Figure 1. Sketch of the system showing the blade three times in the same figure to illustrate a motion sequence of the blade in its second flapwise mode.

co-ordinate system spanned by $\underline{\mathbf{e}}_I$, where $\underline{\mathbf{e}}_I$ holds the three unit vectors $\mathbf{e}_{I1}$, $\mathbf{e}_{I2}$, $\mathbf{e}_{I3}$. A twice underlined character is a matrix, e.g., $\underline{\underline{M}}$.

Rotation of the cross-section about an axis in the cross-sectional plane will be called tilt in order to differentiate between this bending-related motion and a rotation about the longitudinal blade axis.

Only isotropic blade material is considered. Approaches accounting for orthotropic laminate characteristics of rod material have been made (see reference [5]). However, for the blade little information was available about fibre directions; therefore, isotropic material properties were assumed.

2.1. PRINCIPLE OF VIRTUAL WORK

The equations of motion are derived from the principle of virtual work:

$$\delta W = \delta T + \delta U \stackrel{!}{=} 0, \tag{1}$$

where $\delta U = \int_V -\sigma_{ij}\,\delta\varepsilon_{ij}\,\mathrm{d}V$ is the virtual strain energy and $\delta T = \int_V -\varrho\ddot{\mathbf{r}}\cdot\delta\mathbf{r}\,\mathrm{d}V$ is the virtual work of d'Alembert forces. For simplicity, the virtual work of gravitational and dissipative forces is not accounted for.

In the following sections, it is important to remember that in the principle of virtual work a duality exists between forces and stresses on the one hand and deflections and strains on the other. When assuming, for example, that the main stresses in the cross-sectional plain σ_{xx} and σ_{yy} can be neglected and be set to zero, then the respective (variations of the) strains are of no importance for the computation of δU.

2.1.1. *Kinematics*

The unit vectors $(\mathbf{e}_{I1}, \mathbf{e}_{I2}, \mathbf{e}_{I3})^{\mathrm{T}} := \underline{\mathbf{e}}_I$ form an orthogonal inertial right-hand co-ordinate system with $\mathbf{e}_{I1}, \mathbf{e}_{I3}$ spanning a horizontal plane (Figure 1). Cross-sectional deflections of the

blade are conveniently described in a co-ordinate system, which is rigidly connected to the moving blade root. A transformation using matrices $\underline{\underline{D}}_i(\cdot)$ rotates the blade-root co-ordinate system $\mathbf{e}_B$, which is attached to S, by angles $\kappa_i(t)$, $i = 1, 2, 3$ about O, and thus

$$\underline{\mathbf{e}}_B(t) = \underline{\underline{D}}_3(\kappa_3(t))\,\underline{\underline{D}}_2(\kappa_2(t))\,\underline{\underline{D}}_1(\kappa_1(t))\,\underline{\mathbf{e}}_I$$

where

$$\underline{\underline{D}}_1(\alpha) = \begin{bmatrix} 1 & 0 & 0 \\ 0 & \cos(\alpha) & \sin(\alpha) \\ 0 & -\sin(\alpha) & \cos(\alpha) \end{bmatrix}, \qquad \underline{\underline{D}}_2(\alpha) = \begin{bmatrix} \cos(\alpha) & 0 & -\sin(\alpha) \\ 0 & 1 & 0 \\ \sin(\alpha) & 0 & \cos(\alpha) \end{bmatrix},$$

$$\underline{\underline{D}}_3(\alpha) = \begin{bmatrix} \cos(\alpha) & \sin(\alpha) & 0 \\ -\sin(\alpha) & \cos(\alpha) & 0 \\ 0 & 0 & 1 \end{bmatrix} \tag{2}$$

from reference [7] holds. The reference axis R and $\mathbf{e}_{B3}$ are parallel. R is not a particular axis (such as the connection of the centres of mass of all cross-sections would be), but is chosen with some arbitrariness.

B is the origin of the x, y, z co-ordinate system in the blade root. A material blade point $\{x, y, z\}$ is identified by its position vector in the undeformed reference configuration of the blade

$$\mathbf{r}_P^{(0)}(x, y, z; t) = x\,\mathbf{e}_{B1} + y\,\mathbf{e}_{B2} + (b + z)\,\mathbf{e}_{B3}. \tag{3}$$

The crucial question is, what blade deformations have to be accounted for and what co-ordinates should conveniently be used to describe them. The chosen co-ordinates are introduced by following the material points of the cross-section z from their reference position in space to the deflected configuration. To begin with, the displacements $\underline{u} = (u_1(z, t), u_2(z, t), u_3(z, t))^{\mathrm{T}}$ of cross-section z with respect to point $\{0, 0, z\}$ on R are introduced in the $\underline{\mathbf{e}}_B$ co-ordinate system. Co-ordinate u_3 is the displacement of the cross-section in the longitudinal blade direction (extension), u_1 and u_2 are lateral displacements. A new co-ordinate system is introduced which follows the rotations of every cross-section z due to bending and torsion of the blade. The cross-section is tilted by angle $\varphi_1(z, t)$ about $\mathbf{e}_{B1}$, subsequently $\varphi_2(z, t)$ about the resulting 2-axis and then rotated (pitched) $\varphi_3(z, t)$ about the 3-axis. $\varphi_1(z, t)$ rotates points on cross-section z in the y–z plane. For an Euler–Bernoulli beam, this rotation would explicitly be defined to be $\varphi_1 = -\partial u_2/\partial z$, such that cross-sections remain perpendicular to the beam's centre line. Likewise, φ_2 is the tilt-angle associated to bending in u_1. Rotation φ_3 relates to the torsion of the blade.

Using transformations $\underline{\underline{D}}_i$ from equation (2) again, the co-ordinate system attached to cross-section z is

$$\underline{\mathbf{e}}_C(z, t) = [\underline{\underline{D}}_3(\varphi_3(z, t))\,\underline{\underline{D}}_2(\varphi_2(z, t))\,\underline{\underline{D}}_1(\varphi_1(z, t))]\,\underline{\mathbf{e}}_B, \tag{4}$$

such that point $\{x, y, z\}$ from equation (3) holds at this point of the transformation the spatial position

$$\mathbf{r}_P^{(1)}(x, y, z; t) = (b + z)\,\mathbf{e}_{B3} + \underline{u}\,\underline{\mathbf{e}}_B + (x, y, 0)^{\mathrm{T}}\,\underline{\mathbf{e}}_C. \tag{5}$$

The displacement described by co-ordinates u_1, u_2, u_3, φ_1, φ_2, φ_3 is a rigid body motion of the cross-sections. Stopping at this point, a Timoshenko beam model would be obtained or, after further assumptions, an Euler–Bernoulli beam model and a separate torsional rod model.

Warping is an out-of-plane deformation of the cross-section and is thus a function of x and y. It causes an elastic coupling of torsion and flexure. With $\mathbf{e}_{C3}$ being perpendicular

to the cross-section defined by equation (5), a warping function $w(x, y, z; t)$ is chosen as

$$w(x, y, z; t) := \psi_1(z, t)\, xy + \psi_2(z, t)\, x^2 + \psi_3(z, t)\, y^2, \tag{6}$$

such that the deflection of point $\{x, y, z\}$ can be described as

$$\mathbf{r}_P^{(2)}(x, y, z; t) = \mathbf{r}_P^{(1)}(x, y, z; t) + w(x, y, z; t)\, \mathbf{e}_{C3}. \tag{7}$$

Linearization of equation (7) with respect to all dependent co-ordinates yields the displacement field $\Delta\mathbf{r}_P(x, y, z; t) = (\Delta r_x, \Delta r_y, \Delta r_z)^{\mathrm{T}}\, \mathbf{e}_I$, where

$$\begin{aligned}
\Delta r_x &= +(b + z)\, \kappa_2(t) - y\, \kappa_3(t) + u_1(z, t) - y\, \varphi_3(z, t),\\
\Delta r_y &= -(b + z)\, \kappa_1(t) + x\, \kappa_3(t) + u_2(z, t) - x\, \varphi_3(z, t),\\
\Delta r_z &= y\, \kappa_1(t) - x\, \kappa_2(t) + u_3(z, \mathrm{t}) + y\, \varphi_1(z, t) - x\, \varphi_2(z, t)\\
&\quad + xy\, \psi_1(z, t) + x^2\, \psi_2(z, t) + y^2\, \psi_3(z, t).
\end{aligned} \tag{8}$$

The warping function can be interpreted as part of a Taylor series expansion of the cross-sectional deflection in the z direction to second order in x and y.

2.1.2. *Strain–displacement relation*

With displacements (8) given, the linearized strains (see reference [8] can be computed by

$$\begin{aligned}
\varepsilon_{xx} &= \partial\Delta r_x/\partial x, \quad \varepsilon_{yz} = \tfrac{1}{2}(\partial\Delta r_z/\partial y + \partial\Delta r_y/\partial z) = \varepsilon_{zy},\\
\varepsilon_{yy} &= \partial\Delta r_y/\partial y, \quad \varepsilon_{zx} = \tfrac{1}{2}(\partial\Delta r_z/\partial x + \partial\Delta r_x/\partial z) = \varepsilon_{xz},\\
\varepsilon_{zz} &= \partial\Delta r_z/\partial z, \quad \varepsilon_{xy} = \tfrac{1}{2}(\partial\Delta r_x/\partial y + \partial\Delta r_y/\partial x) = \varepsilon_{yx}.
\end{aligned} \tag{9}$$

2.1.3. *Stress–strain relation*

Treating the blade as a slender rod, $\sigma_{xx} \equiv 0$ and $\sigma_{yy} \equiv 0$ may be assumed. From the stress–strain relations (Hook's law, see reference [8]), one obtains

$$\sigma_{zz} = E\, \varepsilon_{zz}, \qquad \sigma_{xy} = 2G\, \varepsilon_{xy}, \qquad \sigma_{xz} = 2G\, \varepsilon_{xz}, \qquad \sigma_{yz} = 2G\, \varepsilon_{yz}, \tag{10}$$

where E, G are Young's modulus of elasticity and shear modulus respectively.

Note that the stress–strain relations also yield the strains $\varepsilon_{xx} \equiv \varepsilon_{yy} = -(E/(2G) - 1)\, \varepsilon_{xx}$, which could be used to compute the resulting in-plane deformations of the cross-section.

2.1.4. *Form functions*

Polynomials in z are chosen as form functions to discretize the blade motion

$$\begin{aligned}
u_i(z, t) &= \sum_{j=1}^{N(ui)} U_{ij}(t) \left(\frac{z}{\ell}\right)^j, \qquad \varphi_i(z, t) = \sum_{j=1}^{N(\varphi i)} \Phi_{ij}(t) \left(\frac{z}{\ell}\right)^j,\\
\psi_i(z, t) &= \sum_{j=1}^{N(\psi i)} \Psi_{ij}(t) \left(\frac{z}{\ell}\right)^j.
\end{aligned} \tag{11}$$

Other form functions such as Legendre-type polynomials are more appropriate, but are not employed here for the sake of simplicity. The time-dependent coefficients of the form functions are the dependent co-ordinates of the blade model.

2.1.5. *Definition of blade geometry*

In order to facilitate the numerical integration over the blade body in equation (1) it is subdivided into hexahedra. First, a number of generating cross-sections of different size and

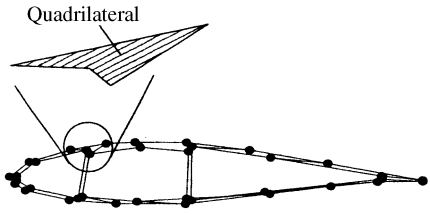

Figure 2. Definition of a cross-section with quadrilaterals. Dots mark the points which define the edges of the quadrilaterals.

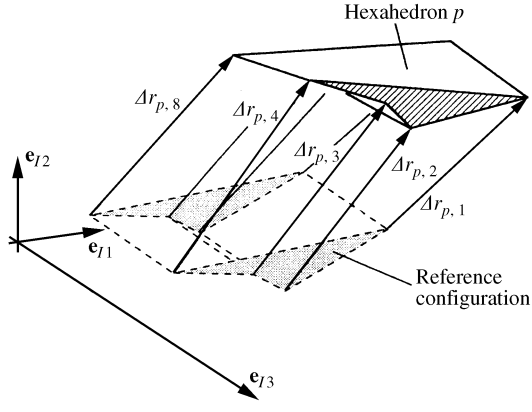

Figure 3. Displacements of the corner points of hexahedron p.

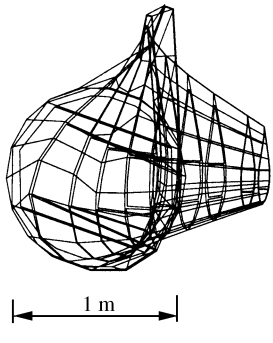

Figure 4. Discretization of the blade geometry.

shape are defined along the blade length. Each of them consists of the same number of quadrilaterals (see Figure 2).

Connecting the edges of a quadrilateral with the respective element on a neighbouring cross-section defines a hexahedron (see Figure 3), which is one "volume element" of the blade. The displacements Δr_{pq}, $q = 1, 2, \ldots, 8$ of the corner points of hexahedron p are explicit functions of the dependant co-ordinates; thus,

$$\Delta r_{pq} = \Delta r_{pq}(\kappa_i(t), U_{ij}(t), \Phi_{ij}(t), \Psi_{ij}(t)).$$

Figure 4 shows the geometry of the blade with generating cross-sections and connecting lines. For clarity, the blade tip is deflected 1 m flapwise from its reference configuration (the

blade is straight in its reference configuration). For simplicity and lack of detailed information, all hexahedra are assumed to consist of the same isotropic material. Using equations (8)–(10), the virtual work (1) for hexahedron p can be given as a function of $\kappa_i(t)$, $u_i(z, t)$, $\varphi_i(z, t)$, $\psi_i(z, t)$ (see Figure 3) and their derivatives using a computer algebra program.

Finally, the virtual work of elastic deformations of the support (stiffnesses K_i, $i = 1, 2, 3$) and d'Alembert forces (moments of inertia J_i, $i = 1, 2, 3$) with respect to $\kappa_1, \kappa_2, \kappa_3$ are included in (1). Then, the elements of the system matrices are extracted from δW by collecting the coefficients of the virtual displacements and the displacements themselves. Their numerical values result from an integration over all hexahedra, which can now be performed numerically. This procedure is equivalent to the assembly of equations of motion in classical FEM programs with the difference, that the dependent co-ordinates are *not* the deflections (or rotations) of the hexahedra corner points, but the co-ordinates κ_i and the coefficients U_{ij}, Φ_{ij}, Ψ_{ij} of the global form functions u_i, φ_i, ψ_i.

2.2. SLAVING WARPING, EXTENSION AND TILT TO THE REMAINING CO-ORDINATES

From the solution of integral (1) over the blade body a system of linear differential equations is obtained—just as in ordinary FE-programs — which can be written as

$$\begin{pmatrix} \underline{\underline{M}}_{ZZ} & \underline{\underline{M}}_{ZQ} \\ \underline{\underline{M}}_{QZ} & \underline{\underline{M}}_{QQ} \end{pmatrix} \begin{pmatrix} \ddot{\underline{Z}} \\ \ddot{\underline{Q}} \end{pmatrix} + \begin{pmatrix} \underline{\underline{K}}_{ZZ} & \underline{\underline{K}}_{ZQ} \\ \underline{\underline{K}}_{QZ} & \underline{\underline{K}}_{QQ} \end{pmatrix} \begin{pmatrix} \underline{Z} \\ \underline{Q} \end{pmatrix} = \underline{0}, \tag{12}$$

where

$$\underline{Z} = \{\kappa_1, \kappa_2, \kappa_3, U_{11}, \ldots, U_{1N(u1)}, U_{21}, \ldots, U_{2N(u2)}, \Phi_{31}, \ldots, \Phi_{3N(\varphi 3)}\}$$

and

$$\underline{Q} = \{U_{31}, \ldots, U_{3N(u3)}, \Phi_{11}, \ldots, \Phi_{1N(\varphi 1)}, \Phi_{21}, \ldots, \Phi_{2N(\varphi 2)}, \Psi_{11}, \ldots, \Psi_{21}, \ldots, \Psi_{3N(\psi 3)}\}.$$

$\underline{Z}$ holds co-ordinates κ_i describing small rotations of the support, U_{1i} and U_{2i} describing lateral blade deflections and Φ_{3i} describing rotation of the blade chord about R. $\underline{Q}$ holds co-ordinates U_{3i} and Φ_{1i}, Φ_{2i} describing longitudinal deflection and tilt of the cross-sections, respectively, as well as the co-ordinates Ψ_{ij} describing out-of-plane deformations of the cross-sections (warping).

The key idea for a reduction of the number of state variables is that the dependant co-ordinates can be separated into one set $\underline{Z}(t)$ dominating the kinetic energy of eigenmodes below a certain chosen frequency f^* and the remaining $\underline{Q}(t)$ above f^*. Eigenmodes above f^* are assumed to be of no practical interest for the problem stated.

Example: For bending of slender beams, the *strain energy* is governed by a longitudinal change in the tilt angle of the cross-sections, represented by $\underline{Q}$. But the contribution of their rotational inertia terms to the *kinetic energy* for low-frequency modes is practically negligible and is governed predominantly by the lateral deflections, represented by $\underline{Z}$.

The kinetic energy related to $\underline{Q}$ dominates eigenmodes in the very high-frequency range and contributes to the lower-frequency modes by a kind of forced compliance motion only. In physical systems where damping is always present, their modes decay very rapidly and do not contribute to the solution of interest. For the solution of the equations of motion, especially when solving as an initial value problem, it is most desirable to eliminate them from the set of minimal co-ordinates.

Neglecting the virtual work of the d'Alembert forces related to $\underline{Q}$ by choosing

$$\underline{\underline{M}}_{ZQ} = \underline{\underline{0}}, \qquad \underline{\underline{M}}_{QZ} = \underline{\underline{0}}, \qquad \underline{\underline{M}}_{QQ} = \underline{\underline{0}},$$

constraint equations between $\underline{Q}$ and $\underline{Z}$ are obtained from equation (12) as

$$\underline{Q} = -\underline{\underline{K}}_{QQ}^{-1}\,\underline{\underline{K}}_{QZ}\,\underline{Z}, \tag{13}$$

which can be interpreted as a kind of "gear" mechanism. The introduction of equation (13) into equation (12) yields

$$\underline{\underline{M}}_{ZZ}\ddot{\underline{Z}} + \underbrace{(\underline{\underline{K}}_{ZZ} - \underline{\underline{K}}_{ZQ}\,\underline{\underline{K}}_{QQ}^{-1}\,\underline{\underline{K}}_{QZ})}_{=:\,\underline{\underline{K}}^*}\,\underline{Z} = \underline{0} \tag{14}$$

where $\underline{\underline{K}}^*$ is the reduced stiffness matrix. The remaining minimal co-ordinates are $\underline{Z}$. For the low-frequency modes, the reduction of the stiffness matrix does not cause a loss of accuracy since all the mechanisms of the original stiffness matrix contribute. The procedure in equation (13) and (14) is similar to that in reference (9).

The equations of motion are solved as an eigenvalue problem.

3. COMPARING MODEL AND EXPERIMENT

3.1. EXPERIMENTS

The experimental modal analysis was performed at Sparkær Blade Test Centre on a 19 m long blade. Three charge accelerometers were used for each of 10 cross-sections of the blade between tip and root. The blade was excited using a heavy hammer with a very soft tip at $z = 11$ m, the hammer force $f(t)$ was measured and the frequency response functions were obtained. Modal mass, damping, stiffness and modeshapes were identified. A detailed description of the measurement set-up and procedure is given in reference [10].

3.2. BLADE MODEL

For the mathematical model used in the following comparison between simulation and experiment, the number of form functions are set to

$$N(u_3) = N(\varphi_1) = N(\varphi_2) = N(\psi_i) = 10, \qquad i = 1, 2, 3$$

and

$$N(u_1) = N(u_2) = N(\varphi_3) = 8.$$

The three rotational springs K_i and moments of inertia J_i present a simple model for the support. The stiffnesses K_i of the test stand were measured by attaching a laser to the support with the laser beam marking a point on a wall at a distance of 25 m. The blade was loaded with a constant force at the tip and from the displacement of the laser point on the wall, the stiffnesses were computed and set to $K_i = 5 \times 10^8$ N m, $i = 1, 2, 3$. Parameter values for the moments of inertia were estimated to be $J_i = 10^3$ kg m^2, $i = 1, 2, 3$.

3.3. COMPARISON

Table 1 compares measured and computed eigenfrequencies. The given mode names describe the predominant motion of the blade.

TABLE 1

Comparison of measured and computed eigenfrequencies

Mode name	Measured e.f./Hz	Computed e.f./Hz
First flap	1·64	1·60
First edge	2·94	3·06
Second flap	4·91	5·01
Third flap	9·73	10·07
Second edge	10·62	11·90
Fourth flap	16·25	17·02
First pitch	22·87	22·31

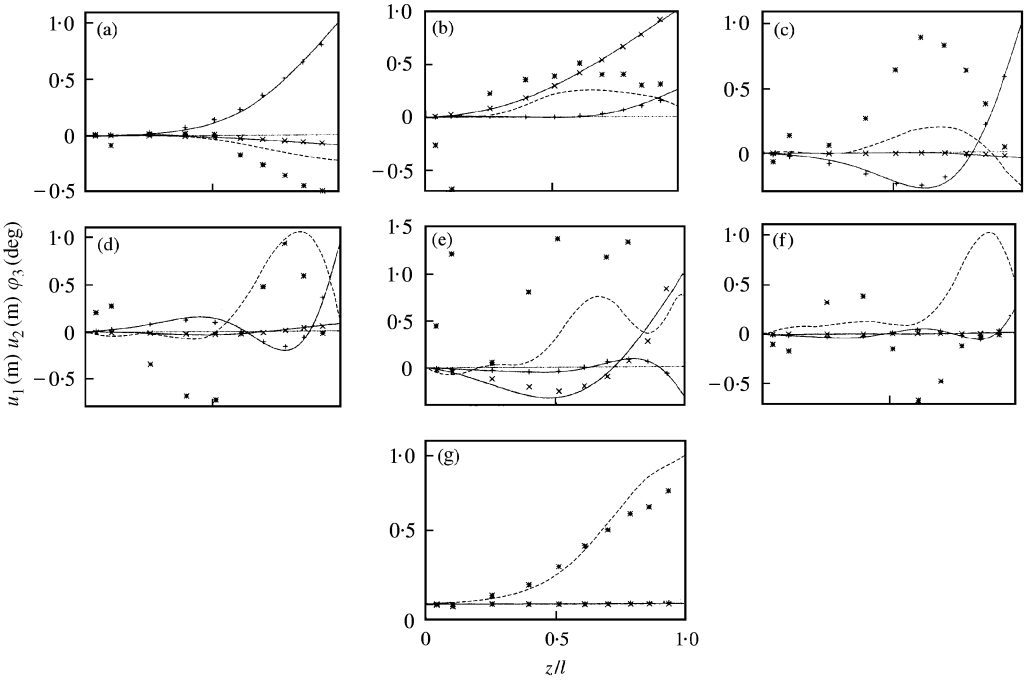

Figure 5. Comparison of measured and computed mode shapes: (a) first flapwise mode; (b) first edgewise mode; (c) second flapwise mode; (d) third flapwise mode; (e) second edgewise mode; (f) fourth flapwise mode; (g) first pitchwise mode. Key for mode shapes: ——, computed u_1; —|—, measured u_1, ·····, computed u_2; ×, measured u_2; – – –, computed φ_3; ×, measured φ_3.

The computed eigenfrequencies approximate the experimentally found results much better than could be expected from a modelling that had to deal with many uncertainties in the system parameters. The modeshapes (Figure 5), however, do not fit as well.

The free multiplier in the measured modeshapes, which scales the blades deflection but leaves the relation between u_1, u_2, φ_3 unchanged, was set to minimize the difference between the measured and computed edge- and flapwise deflections. For nearly all modes in Figure 5, the numerical model approximates the coupling between u_1

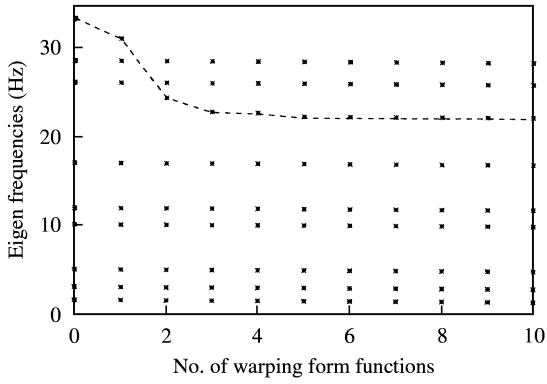

Figure 6. Computed eigenfrequencies of the blade over the number of form functions for ψ_i (broken line indicates first torsional mode).

and u_2 well. The computed chord rotation, however, differs significantly from the measurements, even though the general characteristics of coupling with u_1, u_2 were obtained.

Probably, the unsatisfying agreement between model and experiment can be attributed to the influence of material unisotropy or uncertainties in the modelling of the blade geometry. The simple representation of the test stand in the model or the small static deflections due to gravity are believed to have no relevant influence. However, for initial flapwise tip deflections of 1 m as under operation, the coupling of flexural and torsional deflections increases.

3.4. INFLUENCE OF WARPING

The influence of warping on the modes is investigated. Figure 6 shows the computed eigenfrequencies for the model over the number $N(\psi_i)$, $i = 1, 2, 3$ of form functions used for the ψ_i.

For $N(\psi_i) < 4$, the first pitch eigenfrequency increases significantly, while the other eigenfrequencies remain unaffected. But already at higher numbers of $N(\psi_i)$, the modal coupling between the deflections in φ_3, u_1 and u_2 tends to approximate the measured modeshapes less accurately.

3.5. INFLUENCE OF THE SUPPORT STIFFNESS

In a modal analysis of a wind turbine blade, the support should have little impact on the measured eigenfrequencies and -modes. Using the mathematical model presented, a parameter study with the support stiffness K_1 as variable has been performed (see Figure 7).

K_1 is the rotational stiffness with respect to κ_1 and governs the blade's motion in the vertical plane or edgewise direction. Flapwise eigenfrequencies are only affected for very low values of K_1. About the measured parameter value $K_1 = 5 \times 10^8$ N m, the changes of the eigenfrequencies along K_1 are very small. The test stand can be assumed to be stiff enough to preclude that it adds a significant compliance to the system.

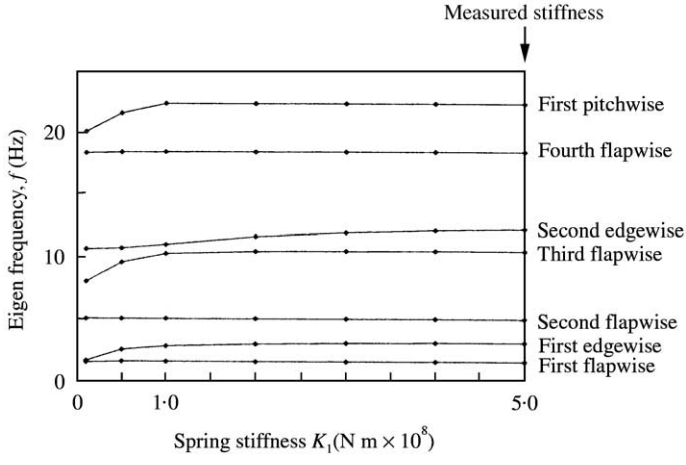

Figure 7. Computed eigenfrequencies of the blade over the support stiffness K_1.

4. CONCLUSION

A rod model for slender, tapered, closed structures is presented and applied to a wind turbine blade. The mathematical model is solved as an eigenvalue problem and the results are compared with an experimental modal analysis.

Even though the general model characteristics (position of nodal points, direction of motion) match quite well, the chord rotation for some modeshapes is significantly underestimated. The question remains as to what assumptions in the modelling process are the main sources of these differences (e.g., parameter uncertainties, unisotropic material, geometry, order of Taylor series expansion in x and y, …).

Nevertheless, the mathematical model presented is a serious alternative to commercial FE methods when computing first estimates for eigenfrequencies and modal shapes. The very few degrees of freedom allow applications for systematic stability investigations and fast solution as an initial value problem. Due to its semi-analytical nature, the model can be, and has been, extended to allow for rotation of the whole blade and the computation of gyroscopic terms (e.g., centrifugal stiffening) and periodic coefficients (see reference [6]).

REFERENCES

1. S. ØYE 1996 in *State of the Art of Aerolastic Codes for Wind Turbine Calculations*, *International Energy Agency*, 28*th Meeting of Experts* (B. M. Pedersen, editor) 71–76. Lyngby: DTU.
2. J. C. HOUBOLT and G. W. BROOKS 1957 NACA: http://naca.larc.nasa.gov/reports/1958/naca-report-1346/. Differential equations of motion for combined flapwise bending, cordwise bending, and torsion of twisted nonuniform rotor blades.
3. S. KRENK and B. JEPPESEN 1989 *Computers & Structures* **32**, 1035–1043. Analytical solution to the dynamic analysis of laminated beams using higher order refined theory.
4. S. Y. BACK and K. M. WILL 1998 *International Journal for Numerical Methods in Engineering* **43**, 1173–1191. A shear flexible element with warping for thin-walled open beams.
5. T. KANT, S. R. MARUR and G. S. RAO 1989 *Composite Structures*. Amsterdam: *Elsevier Science* **40**, 1–9. Analytical solution to the dynamic analysis of laminated beams using higher order refined theory.
6. H. BREMER 1988 *Dynamik und Regelung Mechanischer Systeme*. Stuttgart: B. G. Teubner.

7. M. R. SPIEGEL 1959 *Vector Analysis*. New York: Schaum Publishing Co.
8. K. WASHIZU 1968 *Variational Methods in Elasticity and Plasticity*. Oxford: Pergamon Press; third edition, 1982.
9. R. J. GUYAN 1965 *American Institute of Aeronautics and Astronautics Journal* **3**, 380. Reduction of stiffness and mass matrices.
10. G. LARSEN, M. HANSEN, A. BAUMGART and I. CARLÉN 2000 Risø-R-1181. *Modal Analysis of Wind Turbine Blades*. Roskilde: Risø.